Institute of Paper Science and Technology
Atlanta, Georgia

IPST Technical Paper Series Number 813

An Approximate Analytical Expression for the Probability of Attachment by Sliding

F. Bloom and T.J. Heindel

August 1999

Submitted to
Journal of Colloid and Interface Science

INSTITUTE OF PAPER SCIENCE AND TECHNOLOGY
PURPOSE AND MISSIONS

The Institute of Paper Science and Technology is an independent graduate school, research organization, and information center for science and technology mainly concerned with manufacture and uses of pulp, paper, paperboard, and other forest products and byproducts. Established in 1929, the Institute provides research and information services to the wood, fiber, and allied industries in a unique partnership between education and business. The Institute is supported by 52 North American companies. The purpose of the Institute is fulfilled through four missions, which are:

- to provide a multidisciplinary education to students who advance the science and technology of the industry and who rise into leadership positions within the industry;
- to conduct and foster research that creates knowledge to satisfy the technological needs of the industry;
- to serve as a key global resource for the acquisition, assessment, and dissemination of industry information, providing critically important information to decision-makers at all levels of the industry; and
- to aggressively seek out technological opportunities and facilitate the transfer and implementation of those technologies in collaboration with industry partners.

ACCREDITATION

The Institute of Paper Science and Technology is accredited by the Commission on Colleges of the Southern Association of Colleges and Schools to award the Master of Science and Doctor of Philosophy degrees.

An Approximate Analytical Expression for the Probability of Attachment by Sliding

Frederick Bloom* and Theodore J. Heindel†

* Department of Mathematical Sciences, Northern Illinois University, DeKalb, IL 60115

† Engineering Division, Institute of Paper Science and Technology, 500 10th St., N.W., Atlanta, GA 30318

Suggested Running Title: Attachment by Sliding

Corresponding Author: Theodore J. Heindel
Institute of Paper Science and Technology
500 10th Street, NW
Atlanta, GA 30318-5794
Ph: 404-894-8264
Fax: 404-894-4778
E-mail: ted.heindel@ipst.edu

Abstract

The focus of this paper is on the flotation microprocess of attachment by sliding, considered to be an important microprocesses in flotation separation. A detailed discussion is provided as to which forces are important for this microprocess during flotation deinking. By including the resistive force due to film drainage, the gravitational force, and the flow force between the bubble and particle, and accounting for both Stokes and non-Stokes flow conditions, a closed-form approximation for the probability of attachment by sliding (P_{asl}) has been developed. The expression presented here is a function of fluid properties, bubble and particle physical properties, and the ratio of the initial-to-critical film thickness separating the bubble and particle (h_0/h_{crit}).

Using this result, it is shown that P_{asl} generally decreases with increasing h_0/h_{crit} and increases with increasing bubble and particle radii and particle density. However, local minima are observed. Additionally, the transition from Stokes to non-Stokes flow conditions results in an abrupt transition in the P_{asl} predictions.

Keywords: attachment by sliding; flotation; microprocess probability; thin film dynamics

Introduction

Flotation is a separation process used in many industries including petrochemical refining, water treatment, mineral processing, and paper manufacturing. Gas bubbles are injected into agitated liquid tanks containing one or more suspended solids to be removed. The bubbles preferentially attach to naturally or chemically hydrophobized solid particles, carrying them to the froth layer where they are removed. The particular process of interest here is flotation deinking, a flotation process used in paper manufacturing to remove contaminant particles (e.g., inks and toners) from recovered wastepaper. Flotation cell designs vary with respect to their geometry, operating parameters, and flow configurations. Despite the many design differences, however, all flotation cells operate on similar principles, and in all modern flotation systems, three separate processes take place in tandem:

1. aeration, whereby air bubbles are introduced into the suspension;
2. mixing, where bubbles and particles are intimately mixed to maximize bubble/particle interaction; and
3. separation, where bubbles and bubble/particle aggregates are allowed to separate from the bulk mixture and are skimmed away.

One consistent theme in flotation modeling has been to treat the overall process as a multistage probability process; such an approach is directly tied to the idea of treating the overall flotation mechanism as a sequence of microprocesses. A survey of attempts to model the overall flotation process may be found in (1-7). As for the sequence of microprocesses themselves, these can generally be ordered as follows:

(a) the approach of a particle to an air bubble with the subsequent collision with, or interception of the particle by the bubble (for particles the size of typical ink particles found in flotation deinking, the main focus here is on the zone of possible interaction which is created when the particle approaches to within a sufficiently small distance of the bubble); for recent progress on this aspect of the problem we refer the reader to (8) and the discussions contained therein

(b) the formation of a three-phase contact angle after sliding of the particle along the thin liquid film which separates the particle from the bubble and the subsequent thinning and rupture of this film; and

(c) the stabilization of the bubble/particle aggregate and its transport to the froth layer for removal.

It is widely understood that the flotation microprocess of sliding of the particle over the bubble surface, with a thin liquid (disjoining) film separating the particle from the bubble, is considered important. In this paper we will develop a new expression for P_{asl}, the probability of adhesion by sliding. In order to predict P_{asl}, one must model the particle motion in the flow field of the bubble as it moves (in an assumed circular path) over the surface of the disjoining film and must also model the drainage and subsequent rupture of that film. Indeed, during the sliding process, the disjoining film (assumed to have some initial thickness h_0) may thin down to that critical thickness h_{crit} at which point rupture of the film occurs with the subsequent development of a three-phase contact between the particle, liquid film, and bubble. As the particle slides over the surface of the disjoining film surrounding the bubble, a minimal time τ_i, the so-called induction time, is required in order for the film to thin out to the point where rupture can occur. If τ_{sl} is the 'sliding time' associated with the motion of the particle over the film's surface, then for attachment to occur we must have $\tau_{sl} \geq \tau_i$.

The motion of the particle over the surface of the disjoining film is, of course, governed by a force balance which will be discussed, in detail, below; the various possible forces which can act on the particle during the sliding process are depicted in Fig. 1. The key to the modeling of the force balance governing P_{asl} is the determination of an appropriate expression for F_T, the resistive force which is generated during the drainage of the liquid film surrounding the bubble surface. Expressions for F_T are determined by using the theory of capillary hydrodynamics for thin films; a comprehensive discussion of the situation may be found in (1) along with the derivation of the expression for F_T which will be employed in the present work. We note that the form of F_T used in the model presented below takes into account *only* the (assumed constant) surface (interfacial) tension of the disjoining film and *does not* reflect the influence surfactant concentration may have on London-Van der Waals dispersion (as gauged by the Hamaker constant), electrostatic interactions, or long-range hydrophobic attraction forces.

Theories of thin-film capillary hydrodynamics have been widely discussed in the fluid dynamics literature. The computation of the expression for F_T, which is used in the present work is based on the analysis presented in Derjaguin et al. (9) and related work by these authors, e.g., Rulev and Dukhin (10), which has been referenced in (1) and summarized by Schulze in (4). Analyses similar to that presented in (9) appear in the work of Ruckenstein and Jain (11), in which variations in the surface concentration of surfactant are discussed, Scheludko et al. (12), and Jain and Ivanov (13). A careful discussion of thin film dynamics which incorporates London-Van der Waals dispersion and examines nonlinear effects on film rupture may be found in Williams and Davis (14). Other discussions related to modeling the thinning out of the disjoining film surrounding a bubble during the sliding process may be found in the recent work of Paulsen et al. (15) which also considers the effect of variable surface tension on film rupture. A discussion of the possible role of long-range hydrophobic attraction forces in the thinning and rupture of disjoining films has been presented in some detail by Paulsen et al. (16), as well as in the recent work by Yoon and Mao (6). Particle attachment to a bubble has also been recently summarized by Nguyen et al. (17, 18).

Systems of equations that can be used to model the sliding of a particle over the surface of a disjoining film surrounding a bubble have been presented by Schulze (5, 19). Because of the inclusion of all the forces depicted in Fig. 1 in the analyses presented in (5) and (19), it is not possible to generate a closed form approximate expression for P_{asl} from the equations for $h_p(t)$ and $\varphi_p(t)$ which are presented in these papers; here, $\varphi = \varphi_p(t)$ (see Fig. 2) describes the angular position of the particle at time t, where $\varphi_p(0) = \varphi_0 \equiv \varphi_T$ is the touching angle, and $h_p(t)$ is the height (or thickness) of the disjoining film between the particle and bubble at the current position of the particle at time t. In the present work, we will argue against the inclusion of some of those forces in the force balance equations that have been employed, e.g., in (19), to derive a system of equations for $(\varphi_p(t), h_p(t))$; some of these arguments are predicated on the relative magnitudes of the various forces involved, while others involve considerations related to the physical relevance of particular forces, and the expressions employed for them within the context of the actual problem under consideration.

Discussions of the computation (numerically) of P_{asl}, which are based on computing τ_{sl} and τ_i directly from the equations governing the motion of a particle (over the surface of the disjoining film), and the equations governing the thinning of the disjoining film, respectively, may be found in Dobby and Finch (20) and Schulze (4), as well as in Yoon and Luttrell (7). In (7), what appear to be closed form analytical expressions for P_{asl} are presented for Stokes flow, intermediate flow, and potential flow conditions; these expressions, however, all turn out to depend implicitly on the angle φ^*_{crit}, where φ^*_{crit} is the largest value of the touching angle φ_T, for a given value of h_0, such that film rupture will occur at an angle

$\varphi = \varphi_{crit} \leq \pi/2$. However, $P_{asl} = \sin^2 \varphi^*_{crit}$; therefore, knowledge of φ^*_{crit} allows for a direct computation of P_{asl}, thus, negating the potential utility of the referenced expressions in (7). Indeed, it is believed by the authors that the expression for P_{asl} which is derived here represents the first, analytical, closed-form (albeit, approximate) formula for this key flotation microprocess probability that has appeared in the literature. This model for P_{asl} will be incorporated into an overall model of the flotation separation process currently being developed (1-3,8).

An Analytical Expression for P_{asl}

To begin the analysis (and with reference to Fig. 2), we let $h(x,t)$ be the height of the disjoining film at the position $x = R_B\varphi$ along the bubble surface, where $0 \leq \varphi \leq \frac{\pi}{2}$. Thus,

$$h_p(t) = h(R_B\varphi_p(t), t) \tag{1}$$

As already indicated, $\varphi = \varphi_p(t)$ describes the angular position of the particle at time $t \geq 0$ where $\varphi_p(0) = \varphi_0 \equiv \varphi_T$ is the touching angle. The radial position of the particle at time t is given by

$$r_p(t) = R_B + R_p + h_p(t) \tag{2}$$

A balance of forces in the radial (r) and angular (φ) directions leads to a coupled system of nonlinear ordinary differential equations of the form

$$\left\{ \begin{aligned} \frac{d\varphi_p}{dt} &= f(\varphi_p(t), h_p(t)) \\ \frac{dh_p}{dt} &= g(\varphi_p(t), h_p(t)) \end{aligned} \right. \tag{3}$$

with associated initial data

$$\varphi_p(0) = \varphi_0(\equiv \varphi_T), \; h_p(0) = h_0 \tag{4}$$

Systems of the form [3] and [4] have appeared previously in the literature, e.g., Schulze (19), in connection with the computation of P_{asl}.

At some thickness h_{crit} the liquid film separating the particle from the bubble can be expected to spontaneously rupture. It has been common in the literature to set

$$\varphi_{crit} = \varphi(h_{crit}) \tag{5}$$

and to define

$$\varphi^*_{crit} = \max\{\varphi_0 | \text{ for a given } h_0,\ \varphi_{crit} \leq \frac{\pi}{2}\} \tag{6}$$

Once φ^*_{crit} has been determined, standard arguments (e.g., (3, 7, 19)) lead to the conclusion that

$$P_{asl} = \sin^2 \varphi^*_{crit} \tag{7}$$

Therefore, to determine P_{asl}, one must obtain φ^*_{crit} from the coupled system of nonlinear ordinary differential equations in [3].

The probability of adhesion by sliding, P_{asl}, depends on (i) h_{crit}, (ii) the flow field around the bubble, (iii) the mobility of the bubble surface, (iv) the (relative) particle and bubble sizes R_p and R_B, and (v) the bubble rise velocity v_B. In the present work, our assumptions will be similar to those made, e.g., in Schulze (19):

A1. The particle executes a quasi-stationary motion and moves in an almost circular path across the bubble surface.

A2. $L >> \bar{h}_p$ and $dL/dt >> d\bar{h}_p/dt$, where L is the length of the sliding path, while $\bar{h}_p(t)$ is the average film thickness during the sliding process.

A3. Boundary-layer effects around the bubble surface are ignored.

A4. The tangential fluid velocity u_φ is given by potential flow for the case of an unretarded bubble surface and by the intermediate flow of Yoon and Luttrell (7) in the case of a completely retarded bubble surface.

In addition, we shall make the assumption that

A5. The direction of a rising bubble is the (+) direction while the direction of a settling particle is the (−) direction; this sign convention will be respected with reference to all vectorial quantities (forces, velocities, and accelerations) which enter the discussion in this section. In particular, sgn $v_{ps} = -$sgn v_B, where v_{ps} is the particle settling velocity and, by convention, $v_B > 0$.

In accordance with assumption A1, we ignore inertial effects in modeling the sliding motion of a particle. The tangential particle velocity $v_{p\varphi}^{rel}$ relative to the bubble is, therefore, given by

$$v_{p\varphi}^{rel} = \frac{dL}{dt} \simeq r\frac{d\varphi_p}{dt} = u_\varphi - v_{ps}\sin\varphi \qquad [8]$$

In actuality, as $r_p(t) = R_B + R_p + h_p(t)$, $\dfrac{dL}{dt} = r\dfrac{d\varphi_p}{dt} + \varphi_p\dfrac{dh_p}{dt}$ in [8]; however, the second term on the right-hand side of this equation has been dropped in view of assumption A2, above. In [8], v_{ps} represents the particle settling velocity given by

$$v_{ps} = \lambda\tilde{v}_{ps} \qquad [9]$$

and

$$\tilde{v}_{ps} = -\frac{2R_p^2\,\triangle\rho g}{9\mu_\ell} \qquad [10]$$

$$\lambda \equiv 6\pi\mu_\ell R_p/f \equiv 18Re_p/Ar \qquad [11]$$

We now define the dimensionless particle settling velocity G by

$$G = \frac{v_{ps}}{v_B} \tag{12}$$

By virtue of the sign convention laid down in assumption A5, $G < 0$. In [9]-[11], $\tilde{v}_{ps}$ is the particle settling velocity which corresponds to the case of Stokesian flow while f is the fluid flow friction factor, $\triangle\rho = \rho_p - \rho_\ell$, is the difference of the particle and fluid densities, g is the acceleration due to gravity, and μ_ℓ is the fluid viscosity; also, Re_p is the particle Reynolds number, $Ar = \dfrac{\triangle\rho d_p^3 g}{\rho_\ell \nu_\ell^2}$ is the Archimedes number where $d_p = 2R_p$ is the particle diameter and ν_ℓ is the fluid kinematic viscosity, $\nu_\ell = \mu_\ell/\rho_\ell$. For the Stokesian case $\lambda = 1$. In fact, for Stokesian particles it is well know that $f = 6\pi\mu_\ell R_p$ as the drag force is given by $\mathbf{F}_d = 6\pi\mu_\ell R_p \mathbf{v}_p$ with $\mathbf{v}_p$ the particle velocity. For non-Stokesian particles we have, in general, $\mathbf{F}_d = f\mathbf{v}_p$ while the coefficient of drag, C_D, is defined to be

$$C_D \equiv \frac{|\mathbf{F}_d|}{\frac{1}{2}\rho_\ell |\mathbf{v}_p|^2 \pi R_p^2} \tag{13}$$

In view of the definition of $\mathbf{F}_d$ in terms of f,

$$C_D = \frac{f}{\frac{1}{2}\rho_\ell |\mathbf{v}_p| \pi R_p^2} \tag{14}$$

In the Stokesian case, with $f = 6\pi\mu_\ell R_p$ and $C_D = C_D^{st}$, [14] yields

$$C_D^{st} = 12\nu_\ell / R_p |\mathbf{v}_p| \tag{15}$$

If we define, in the usual manner, the Reynolds number for the particle to be

$$Re_p = \frac{2R_p|\mathbf{v}_p|}{\nu_\ell} \tag{16}$$

then [15] and [16] yield the widely known result (e.g., (21)) that $C_D^{st} = 24/Re_p$. In the general case, however, it is easily seen that [14] and [16] combine so as to yield

$$C_D = \frac{4f}{(\pi\mu_\ell R_p)Re_p} \tag{17}$$

It is generally accepted that $C_D = C_D^{st} = 24/Re_p$ holds for $Re_p < 2$ (21). For the situation in which inertial forces acting on the particle are ignored, the particle velocity corresponds to the particle settling velocity ($\mathbf{v}_p = \mathbf{v}_{ps}$). In this case it can be demonstrated (i.e., (21)) that

$$C_D Re_p^2 = \frac{4}{3} Ar \qquad [18]$$

For the Stokes' law range ($Re_p < 2$), the use of $C_D = C_D^{st} = \dfrac{24}{Re_p}$ in [18] leads to $Re_p = \dfrac{Ar}{18}$. In the intermediate or transitional range for which $2 < Re_p < 500$, empirical results must be used; from the results reported in (21) one may infer that

$$C_D = \frac{18.5}{Re_p^{0.6}}, \quad 2 < Re_p < 500 \qquad [19]$$

the use of which in [18] yields

$$Re_p = 0.152 Ar^{0.715}, \quad 2 < Re_p < 500 \qquad [20]$$

Hence, [20] can be used in [11] and [9] to determine the actual particle settling velocity when it deviates from Stokes flow, and λ is a measure of this deviation. The sensitivity of λ to changes in particle radius and density is shown in Fig. 3. Particles typical of those found in flotation deinking generally fall in the range $1.1 \lesssim \rho_p \lesssim 1.6\ g/cm^3$ and $20 \lesssim R_p \lesssim 300\ \mu m$, whereas those found in mineral processing typically encompass $2 \lesssim \rho_p \lesssim 10\ g/cm^3$ and $1 \lesssim R_p \lesssim 20\ \mu m$. Particles following Stokes flow conditions correspond to $\lambda = 1$. There is a particular particle radius-density combination at which λ deviates from $\lambda = 1$, coinciding with the transition point of $Re_p = 2$ (i.e., [20]). Knowledge of this discontinuity will be important when analyzing P_{asl} predictions. In general, for particles common to mineral flotation, Stokes flow conditions are followed. In contrast, for particles found in flotation deinking, the deviation from Stokes flow conditions can be significant for very large particle radii.

In analyzing particle motion during sliding, Schulze (5, 19) begins by taking as the form of the equation representing balance of forces in the tangential direction the relation

$$|\boldsymbol{F}_{g\varphi}| - |\boldsymbol{F}_{w\varphi}| = 0 \tag{21}$$

where $\boldsymbol{F}_{g\varphi}$ is the tangential component of the weight of the particle while $\boldsymbol{F}_{w\varphi}$ is the resistive (or drag) force acting on the particle in the vicinity of the bubble surface; this latter force depends on the nature of the flow field and on the degree of bubble coverage with surfactant molecules. In all that follows we shall denote, by the corresponding scalar, the magnitude of an indicated force, i.e., $|\boldsymbol{F}_{g\varphi}| = F_{g\varphi}$, etc. For the force component $F_{w\varphi}$ near a completely retarded bubble ($\bar{h}_p/R_p > 10^{-3}$) Goldman et al. (22) have shown that for the case of a Stokes flow about the bubble

$$\tilde{F}_{w\varphi} \simeq \frac{16}{5}\pi\mu_\ell v_{p\varphi}^{rel} R_p \Big| \ln\left(\frac{h_p}{R_p}\right) \Big|$$

By modifying the analysis in (22) to cover those cases in which the dimensionless friction factor $\lambda \equiv 6\pi\mu_\ell R_p/f \neq 1$, it is easy to deduce that the analysis in (22) leads to

$$F_{w\varphi} \simeq \frac{16}{5\lambda}\pi\mu_\ell v_{p\varphi}^{rel} R_p \Big| \ln\left(\frac{h_p}{R_p}\right) \Big| \tag{22}$$

For $F_{g\varphi}$ one has

$$F_{g\varphi} = \frac{4}{3}\pi R_p^3 \,\triangle\rho g \sin\varphi_p \tag{23}$$

Substitution of [22] and [23] into [21], and subsequent simplification, yields upon solving for $v_{p\varphi}^{rel}$

$$v_{p\varphi}^{rel} \equiv \frac{v_{ps}\sin\varphi_p}{(\frac{8}{15})|\ln(h_p/R_p)|} \tag{24}$$

However, for a neutrally buoyant particle, it follows from [9] and [18] that $v_{ps} = 0$; in this case [24], which is a direct consequence of the assumed form of the tangential balance law in Schulze (5, 19), yields $v_{p\varphi}^{rel} = 0$ which is, of course, nonsense because it implies that the particle never approaches the bubble. In fact, if $v_{ps} = 0$ then, by virtue of [8], $v_{p\varphi}^{rel} = u_\varphi$ where, for an assumed intermediate flow over the bubble surface, it follows from the work of Yoon and Luttrell (7) that

$$\begin{aligned} u_\varphi &= v_B\left(1 - \frac{3R_B}{4r} - \frac{R_B^3}{4r^3}\right)\sin\varphi_p(t) \\ &\quad + v_B Re_B^*\left(\frac{R_B}{r} + \frac{R_B^3}{r^3} - \frac{2R_B^4}{r^4}\right)\sin\varphi_p(t) \\ &\equiv v_B g(r)\sin\varphi_p(t) \end{aligned} \qquad [25]$$

with $Re_B^* = \frac{1}{15}Re_B^{0.72}$, and

$$g(r) = \left(1 - \frac{3R_B}{4r} - \frac{R_B^3}{4r^3}\right) + Re_B^*\left(\frac{R_B}{r} + \frac{R_B^3}{r^3} - \frac{2R_B^4}{r^4}\right) \qquad [26]$$

The contradiction we have arrived at above, in the case where $v_{ps} = 0$, has resulted, of course, from the form [21] of the tangential force balance employed in (5, 19); the correct form of the force balance in the tangential direction must include the angular component $\boldsymbol{F}_{u\varphi}$ of the fluid flow force no matter how small in magnitude this force is in comparison with the other force magnitudes in the balance equation. In deriving an expression for P_{asl} in this section we will not need to make use of a force balance equation for the sliding particle in the tangential direction; as will be seen in the analysis to follow, a judicious use of [8], in combination with the appropriate form of the force balance equation in the radial direction, suffices to produce the desired approximate analytical expression for P_{asl}. The use of both a radial and tangential force balance equation would be needed only if we were actually interested in monitoring the evolution in time of both the film thickness and the angular position of the particle.

We now consider the form assumed by the quasi-static force balance in the radial direction; the most general structure for such an equation, under the present set of assumptions relative to the motion of the particle, is

$$-F_{gr} + F_c + F_T - F_{ur} + F_L = 0 \tag{27}$$

where F_{gr} is the magnitude of the component of the particle weight in the radial direction, F_c is the magnitude of the centrifugal force exerted on the particle, F_T is the magnitude of the resistive force generated during the drainage of the disjoining film, F_{ur} is the magnitude of the radial component of the flow force acting on the particle in the vicinity of the bubble surface, and F_L is the magnitude of the lift force.

The magnitude of the component, in the radial direction, of the particle weight, F_{gr}, is easily computed as

$$F_{gr} = \frac{4}{3}\pi R_p^3 \,\triangle\rho g \cos\varphi_p(t) \tag{28}$$

while the magnitude of the centrifugal force, F_c, acting on the particle has the form

$$F_c = \frac{4}{3r}\pi R_p^3 \,\triangle\rho (v_{p\varphi}^{rel})^2 \tag{29}$$

with $r = R_p + R_B + h_p(t)$.

In, e.g., (5) and (19), Schulze has used a classical result of Saffman (23) to express the magnitude of the lift force experienced by a particle as it slides over the disjoining film which separates the particle from a bubble; the result in question has the form

$$F_L = 3.24 \mu_\ell R_p v_{p\varphi}^{rel} \sqrt{Re_S} \tag{30}$$

where $v_{p\varphi}^{rel}$ is given by [8] and Re_S is the Reynolds number of shear which is defined to be

$$Re_S = \frac{4R_p^2}{\nu_\ell}\frac{\partial u_\varphi}{\partial r} \tag{31}$$

The result given by [30] was derived in (23) for flows at small but nonzero Reynolds numbers Re (i.e., spheres moving through a very viscous liquid). Most theoretical attempts to explain lift (see Clift et al. (24) for a survey of such efforts) have focused on flows at small but nonzero Re and have used the technique of matched asymptotic expansions in order to obtain approximate results such as [30]. The approximate result [30] was also derived in (23) by using the technique of matched asymptotic expansions and it is specifically noted there that the derived expression for the magnitude of F_L becomes invalid for large values of $v_{p\varphi}^{rel}$ because a key sequence of steps in the analysis requires that

$$v_{p\varphi}^{rel} << \sqrt{\nu_\ell \frac{\partial u_\varphi}{\partial r}} \qquad [32]$$

By virtue of [25], $u_\varphi = v_B g(r) \sin\varphi$, where $g(r)$ is defined by [26], so that

$$\frac{\partial u_\varphi}{\partial r} = v_B g'(r) \sin\varphi \qquad [33]$$

with

$$\begin{aligned} g'(r) &= \frac{3}{4}\left(\frac{R_B}{r^2} + \frac{R_B^3}{r^4}\right) \\ &+Re_B^*\left(- \frac{R_B}{r^2} - \frac{3R_B^3}{r^4} + \frac{8R_B^4}{r^5}\right) \end{aligned} \qquad [34]$$

Using [8] and [33], and the fact that $u_\varphi = v_B g(r) \sin\varphi$ in [32], we see that this latter requirement is equivalent to

$$(v_B g(r) - v_{ps}) \sin\varphi << \sqrt{\nu_\ell v_B g'(r) \sin\varphi} \qquad [35]$$

with $g(r)$ given by [26] and $g'(r)$ by [34]. By employing physical and geometrical parameters in ranges that are typical for spherical particles and spherical air bubbles in a flotation deinking system, and estimating $r \simeq R_B + R_p$, Fig. 4 shows that [35] is violated except when $\varphi_p(t) \approx 0$, which corresponds to a particle approaching a bubble on the stagnation streamline. Therefore, the application of the expression [30] for F_L is invalid under the present circumstances. It should be noted that [35] is valid if R_p is small ($\sim 1\ \mu m$) and ρ_p is large ($\sim 7\ g/cm^3$), conditions common in mineral flotation.

In an interesting paper, Mileva (25) has studied the feasibility of including the result for F_L, which was given by Saffman (23), in the radial force balance which governs the motion of a solid particle in the boundary layer of a rising bubble. In (25) the flow around the bubble is not modeled by the intermediate flow of Yoon and Luttrell (7) but, rather, by the boundary layer part of Moore's solution (26) for spherical gas bubbles rising steadily through a liquid of low viscosity. It is concluded by the author in (25) that "the major forces carrying the particles towards the bubble's surface are the gravity and the hydrodynamic driving forces $\cdots$ if the flow field is modeled by potential (flow), or by Stokes' equations, the hydrodynamic driving force plays a decisive role and gravity is only a correction factor. The migration force of Saffman's type is a first-order correction to the other two forces pressing the particle towards the bubble's surface $\cdots$ beside the drag force, the centrifugal force also hampers the mutual approach; it is, however, two orders of magnitude smaller than the first-order correction F_L and can be neglected in the force balance."

The work of Mileva (25) supports the philosophy of retaining only F_T and F_{ur} in the quasi-static radial force balance equation [27] and further evidence to that effect appears in the work of Luttrell and Yoon (27), and Dobby and Finch (20); however, the conclusions in (25) may be limited by the same considerations that have been raised earlier, i.e., the essential applicability, in a specific situation, of the Saffman result [30] for F_L.

In Dobby and Finch (20), the computation of P_{asl} is accomplished by estimating the values of τ_i and τ_{sl}. The values of τ_{sl} and τ_i in (20) are computed by ignoring any possible lift force F_L as well as inertial effects; as the authors of (20) note, "the particle actually experiences a velocity gradient across its dimension. This gradient will impart spin to the particle the consequences of which are ignored here. Also ignored are possible particle bounce and inertia effects; detailed analysis through trajectory calculations indicate that these factors are not very important and this model fitted the experimental results of Schulze and Gottschalk (28)." Finally, in (29), McLaughlin has considered the motion of a small, rigid sphere in a linear shear flow, extending Saffman's analysis to those asymptotic cases in which the particle Reynolds number based on its slip velocity is comparable with, or larger than, the square root of the particle Reynolds number based on the velocity gradient. In all the cases considered in (29), the particle Reynolds numbers are assumed to be small compared to unity. It was shown, in (29), that as the Reynolds number based on particle slip velocity becomes larger than the square root of the Reynolds number based on particle shear rate, the magnitude of the inertial migration velocity rapidly decreases to very small values thus suggesting, again, that the lift force in such a situation plays only a minor role in the force balance [27].

To determine the hydrodynamic drag force, F_{ur} must be modified from the form displayed in (27), which holds in Stokes flow, to $F_{ur} = f|u_r|$, where f is the friction factor for the flow and u_r is the radial component of the fluid velocity for an intermediate flow in the vicinity of the bubble surface. As we have indicated, in general

$$f = \frac{\pi \mu_\ell R_p}{3}\left(\frac{Ar}{Re_p}\right) \qquad [36]$$

where Ar is the Archimedes number and Re_p is the particle Reynolds number so that for Stokesian particles $Re_p = \dfrac{Ar}{18}$ and we recover the fact that $f = 6\pi\mu_\ell R_p$. Alternatively, we may introduce the dimensionless friction factor $\lambda \equiv 18 Re_p/Ar$ and write that

$$f = \frac{6\pi \mu_\ell R_p}{\lambda} \qquad [37]$$

Therefore, F_{ur} assumes the form

$$F_{ur} = \frac{6\pi \mu_\ell R_p}{\lambda}|u_r| \qquad [38]$$

with u_r (as given by Yoon and Luttrell (7) for intermediate flow in the vicinity of the bubble surface) having the form

$$u_r = v_B k(r) \cos\varphi_p \qquad [39]$$

with

$$k(r) = -\left\{\left(1 - \frac{3R_B}{2r} + \frac{R_B^3}{2r^3}\right) + 2Re_B^* \left(\frac{R_B^4}{r^4} - \frac{R_B^3}{r^3} - \frac{R_B^2}{r^2} + \frac{R_B}{r}\right)\right\} \qquad [40]$$

Combining [39] with [38] we have

$$F_{ur} = \frac{6\pi\mu_\ell R_p v_B}{\lambda} |k(r)| \cos\varphi_p \qquad [41]$$

where $k(r)$ is given by [40] with $r = R_B + R_p + h_p$.

Comparing the magnitudes of the hydrodynamic drag force, F_{ur}, the gravitational force, F_{gr}, and the centrifugal force, F_c, for conditions common to flotation deinking, results in F_c being several orders of magnitude less than F_{ur} and F_{gr} and can be neglected in the force balance [27]. Sample results from this force balance are shown in Fig. 5 for a range of particle radii. Luttrell and Yoon (27) and Dobby and Finch (20) have assumed that $|F_{gr} - F_c| << F_{ur}$, but as shown in Fig. 5, this assumption is not applicable for flotation deinking. It is true that $F_{gr} < F_{ur}$ for most conditions, but the magnitudes of these forces differ by a factor of five or less. We will include F_{gr} in our analysis. Therefore, [27] can be rewritten as

$$F_T = F_{ur} + F_{gr} \qquad [42]$$

In this paper, the following expression will be employed for the magnitude of the resistive force F_T which is generated during drainage of the disjoining film:

$$F_T = \frac{6\pi\mu_\ell R_p^2 v_{pr}}{h_p C_B} \qquad [43]$$

where C_B (Schulze's notation, e.g., (5)) varies between one (for a completely immobilized or rigid bubble surface) and four (for an unrestrained bubble surface) and, thus, characterizes the degree of immobilization of the bubble surface due to the influence of the adsorption layer of surfactant on the bubble surface. The expression [43] for F_T is a consequence of the theory of capillary hydrodynamics; it has been derived, for the case $C_B = 4$, in Bloom and Heindel (1), as well as in Schulze (4), and Derjaguin et al. (9), by computing the integral of the disjoining pressure P_σ over the bubble surface. In particular, [43] is a consequence of working with that part of the capillary pressure which depends on surface tension σ only and does not take into consideration either London-Van der Waals dispersion or electrostatic interactions; it also does not include the effects of variable interfacial tension due to possible variations in surfactant levels. These effects preclude a closed-form solution but are of continued interest to the authors.

Returning to [43] and noting that

$$v_{pr} = -\frac{dr}{dt} = -\frac{dh_p}{dt} \qquad [44]$$

we have

$$F_T = -\frac{6\pi\mu_\ell R_p^2}{C_B}\frac{1}{h_p}\frac{dh_p}{dt} \qquad [45]$$

With regard to [45] we note that during the course of film thinning, prior to rupture, $\frac{dh_p}{dt} < 0$ so that [45] indeed represents the magnitude of $\boldsymbol{F}_T$.

Therefore, as a consequence of [42], [41], [28], and [45], the quasi-static force balance in the radial direction assumes the form

$$\frac{6\pi\mu_\ell R_p^2}{C_B h_p}\frac{dh_p}{dt} = -\left(\frac{6\pi\mu_\ell R_p}{\lambda}v_B|k(r)| + \frac{4}{3}\pi R_p^3 \triangle \rho g\right)\cos\varphi_p \qquad [46]$$

where $k(r)$ is given by [40] with $r = R_B + R_p + h_p$. Simplifying [46] we obtain the equation

$$\frac{1}{h_p}\frac{dh_p}{dt} = -\frac{C_B}{R_p}\left(\frac{v_B}{\lambda}|k(r)| - \tilde{v}_{ps}\right)\cos\varphi_p \qquad [47]$$

with $\tilde{v}_{ps}$ the particle settling velocity for Stokes flow as given by [10]. By virtue of [8] and [25]

$$r\frac{d\varphi_p}{dt} = (v_B g(r) - v_{ps})\sin\varphi_p \qquad [48]$$

where $g(r)$ is given by [26]. Therefore,

$$r\frac{d\varphi_p}{dh_p}\frac{dh_p}{dt} = (v_B g(r) - v_{ps})\sin\varphi_p \qquad [49]$$

If we now eliminate $\frac{dh_p}{dt}$ between [47] and [49] we are easily led to the relation

$$\frac{d\varphi_p}{dh_p} = \frac{-(v_B g(r) - v_{ps})\tan\varphi_p}{\left(\frac{C_B}{R_p}\right) r(r-(R_B+R_p))\left[\frac{v_B}{\lambda}|k(r)| - \tilde{v}_{ps}\right]} \qquad [50]$$

where we have used the fact that $h_p = r - (R_B + R_p)$. As a direct consequence of [50] it follows that

$$\frac{dh_p}{d\varphi_p} = \frac{1}{(d\varphi_p/dh_p)} < 0 \qquad [51]$$

indicating that film thinning is proceeding as the particle executes its sliding motion.

We will integrate the differential equation [50] by making the change of independent variable $h_p \to r = R_B + R_p + h_p$ in [50], in which case $\frac{d\varphi_p}{dh_p} = \frac{d\varphi_p}{dr}\frac{dr}{dh_p} \equiv \frac{d\varphi_p}{dr}$ and [50] becomes

$$\cot\varphi_p \frac{d\varphi_p}{dr} = A(r) \qquad [52]$$

with

$$A(r) = \frac{v_{ps} - v_B g(r)}{\left(\frac{C_B}{R_p}\right) r(r-(R_B+R_p))\left[\frac{v_B}{\lambda}|k(r)| - \tilde{v}_{ps}\right]} \qquad [53]$$

Integrating [52] from φ_0 to φ_{crit}, on the left-hand side of the equation, and from $R_B+R_p+h_0$ to $R_B + R_p + h_{crit}$, on the right-hand side of the equation, we obtain

$$\ln\left\{\frac{\sin\varphi_{crit}}{\sin\varphi_0}\right\} = Q(h_0, h_{crit}, R_B + R_p) \qquad [54]$$

where

$$Q(h_0, h_{crit}, R_B + R_p) = \int_{R_B+R_p+h_{crit}}^{R_B+R_p+h_0} \frac{(v_B g(r) - v_{ps})}{\left(\dfrac{C_B}{R_p}\right) r(r - (R_B + R_p)) \left[\dfrac{v_B}{\lambda}|k(r)| - \tilde{v}_{ps}\right]} dr \qquad [55]$$

From [54] we readily obtain

$$\varphi_{crit} = \sin^{-1}\left((\sin\varphi_0)e^{Q}\right) \qquad [56]$$

Hence, the solution given by [56] is of the form

$$\varphi_{crit} = \varphi_p(h_{crit}; h_0, \varphi_0) \qquad [57]$$

Equation [57] defines, for fixed h_0 and h_{crit}, a mapping

$$\Phi_p : \varphi_0 \longrightarrow \varphi_{crit} \qquad [58]$$

If h_{crit} is fixed, but h_0 varies, then the mapping in [58] can be considered to be parametrized by h_0, i.e.,

$$\Phi_{p,h_0} : \varphi_0 \longrightarrow \varphi_{crit} \qquad [59]$$

Thus, corresponding to [6] we would have

$$\varphi^*_{crit} = \max\left\{\varphi_0 \middle| \Phi_{p,h_0}(\varphi_0) \leq \frac{\pi}{2}\right\} \qquad [60]$$

However, for an assumed symmetrical flow around the bubble it may be argued that for a fixed h_0, Φ_{p,h_0} is both continuous and monotone so that, in fact,

$$\varphi^*_{crit} = \max\left\{\varphi_0 \middle| \quad \text{for a given } h_0, \varphi_{crit} = \frac{\pi}{2}\right\} \qquad [61]$$

By virtue of the continuity and monotonicity of Φ_{p,h_0}, for fixed h_0, it follows that Φ_{p,h_0} is invertible, that Φ^{-1}_{p,h_0} is continuous, and

$$\varphi^*_{crit} = \Phi^{-1}_{p,h_0}\left(\frac{\pi}{2}\right) \qquad [62]$$

It follows as a consequence of [56] and [62] that

$$\begin{aligned}\varphi^*_{crit} &= \max\left\{\varphi_0 \,\middle|\, \sin^{-1}(e^Q \sin\varphi_0) = \frac{\pi}{2}\right\} \\ &= \sin^{-1}(e^{-Q})\end{aligned} \tag{63}$$

In view of the structure of [55], the fact that both $v_{ps} \leq 0$ and $\tilde{v}_{ps} \leq 0$, as well as the fact that $h_{crit} \leq h_0$, we see that $Q(h_0, h_{crit}, R_B + R_p) \geq 0$ with

$$Q(h_0, h_{crit}, R_B + R_p) = 0 \Leftrightarrow h_o = h_{crit} \tag{64}$$

Also, in view of the continuity of $g(r)$ and $|k(r)|$ in [55], if $h_{crit} \approx h_0$ then $Q \approx 0$ in which case, by [63], $\varphi^*_{crit} \approx \dfrac{\pi}{2}$ and $P_{asl} = \sin^2 \varphi^*_{crit} \approx 1$. As $P_{asl} = \sin^2 \varphi^*_{crit}$ and, $\varphi^*_{crit} = \sin^{-1}(e^{-Q})$, it follows that

$$P_{asl} = e^{-2Q} \tag{65}$$

Returning to [55] and noting that, for the application at hand, the difference $h_0 - h_{crit}$ is very small, we may approximate Q by

$$Q \simeq \frac{v_B g(R_B + R_p + h_{crit}) - v_{ps}}{\left(\dfrac{C_B}{R_p}\right)(R_B + R_p + h_{crit})\left[\dfrac{v_B}{\lambda}|k(R_B + R_p + h_{crit})| - \tilde{v}_{ps}\right]}\left(\frac{h_0}{h_{crit}} - 1\right) \tag{66}$$

Making the further approximation in [66] that

$$R_B + R_p + h_{crit} \simeq R_B + R_p \tag{67}$$

and noting that $G < 0$, we are led to the approximate analytical relation

$$Q \simeq \left(\frac{\lambda}{C_B}\right)\frac{R_p}{R_B + R_p}\left\{\frac{g(R_B + R_p) - G}{|k(R_B + R_p)| - G}\right\}\left(\frac{h_0}{h_{crit}} - 1\right) \tag{68}$$

As $P_{asl} \simeq e^{-2Q}$ we may make the following observations based on the structure of Q in [68]:

(i) If we fix h_0 then as h_{crit} decreases, $\dfrac{h_0}{h_{crit}}$ increases, as does $\left(\dfrac{h_0}{h_{crit}} - 1\right)$; thus, Q also increases in which case P_{asl} decreases.

(ii) As C_B increases (from one to four), Q decreases and, thus, P_{asl} increases. However, this result must be viewed cautiously as h_{crit} and h_0 will both vary with C_B.

(iii) As λ increases, Q increases and P_{asl} decreases.

Combining [65] and [68] the final approximate expression for P_{asl}, which follows from the analysis described above, is:

$$P_{asl} = exp\Big[-2\left(\frac{\lambda}{C_B}\right)\left(\frac{R_p}{R_B+R_p}\right)\left\{\frac{g(R_B+R_p)-G}{|k(R_B+R_p)|-G}\right\}\left(\frac{h_0}{h_{crit}}-1\right)\Big] \qquad [69]$$

where $g(r)$ is given by [26], $k(r)$ by [40], C_B, $1 \le C_B \le 4$, gauges the mobility of the bubble surface, while $\lambda \equiv \dfrac{18Re_p}{Ar}$ gauges, by virtue of [37], the deviation of the friction factor f from the usual friction factor for Stokes flow; for $2 < Re_p < 500$ the empirical relation $Re_p = 0.152Ar^{0.715}$ may be used to compute λ.

As a special case of [69] we may obtain an approximate expression for P_{asl} which holds for Stokes flow around, say, a bubble which is idealized to have a rigid (or completely immobilized) surface; in this situation $\lambda = 1$, $C_B = 1$, and we set $Re_B = 0$. Then $G = \tilde{G}$ where

$$\tilde{G} = \frac{\tilde{v}_{ps}}{v_B} \qquad [70]$$

with

$$\tilde{v}_{ps} = -\frac{2R_p^2 \triangle\rho g}{9\mu_\ell} \qquad [71]$$

the particle settling velocity for Stokes flow, while $g(r)$, $k(r)$ reduce, respectively, to

$$\tilde{g}(r) = 1 - \frac{3R_B}{4r} - \frac{R_B^3}{4r^3} \qquad [72]$$

and

$$\tilde{k}(r) = -\left(1 - \frac{3R_B}{2r} + \frac{R_B^3}{2r^3}\right) \qquad [73]$$

Thus, P_{asl} may, in this case, be approximated by

$$\tilde{P}_{asl} = exp\left[-2\left(\frac{R_p}{R_B + R_p}\right)\left\{\frac{\tilde{g}(R_B + R_p) - \tilde{G}}{|\tilde{k}(R_B + R_p)| - \tilde{G}}\right\}\left(\frac{h_o}{h_{crit}} - 1\right)\right] \qquad [74]$$

We now have an approximate expression for P_{asl} for intermediate flow or Stokes flow conditions. Since most flotation deinking systems typically operate in intermediate flow conditions, selected predictions will now be presented for this case.

Numerical P_{asl} Predictions

In performing the calculations to predict P_{asl}, certain parameters must be known. In our calculations, we assumed that all fluid properties correspond to those of water. Particle density must also be specified, and for most calculations, we assumed $\rho_p = 1.3\ g/cm^3$, which approximates that of toner particles (30).

The bubble surface mobility coefficient, C_B, has been shown to vary between 1 and 4, depending on the concentration of surface active agents in the system. For pure water, $C_B = 4$. However, in deinking operations, the system is contaminated with surface active agents. In this case, the bubble surface is more likely to be rigid, which corresponds to $C_B = 1$. This value was used in our calculations and is a good approximation of a deinking system.

The bubble rise velocity must also be specified for our P_{asl} predictions, and is known to be a function of bubble radius (24). In our calculations, we assumed the system to be water contaminated with surface active agents. The data presented in Clift et al. for air bubbles rising in water (i.e., see Fig. 7.3 in (24)) was curve-fitted to yield the following relationships for bubble rise velocity:

$$v_B = 230 d_B^{1.11} \qquad 0.0002\ m \leq d_B < 0.001\ m \qquad [75]$$

$$v_B = -9.11 \times 10^7 d_B^4 + 2.20 \times 10^6 d_B^3 - 1.84 \times 10^4 d_B^2 + 7.03 \times 10^1 d_B + 5.12 \times 10^{-2} \qquad 0.001\ m \leq d_B \leq 0.01\ m \quad [76]$$

where d_B is the bubble diameter ($= 2R_B$) and measured in meters. The transition from one correlation to the other at $d_B = 0.001\ m$ ($R_B = 0.5\ mm$) corresponds to a change in bubble shape from spherical to ellipsoidal. Although we assume the bubble in our model to be spherical for all conditions, and recent bubble visualization work reveals the bubble remains spherical at larger equivalent diameters in a fiber suspension (31, 32), we do not know what the bubble rise velocity is in a fiber suspension. Therefore, the correlations determined above from the Clift et al. data will be used as a first approximation.

The bubble and particle radius must also be designated in the P_{asl} calculations. These values were varied between $0.1\ mm \leq R_B \leq 5\ mm$ and $1\ \mu m \leq R_p \leq 500\ \mu m$, which encompass expected ranges in flotation deinking operations.

Finally, the ratio of initial to critical film thickness, h_0/h_{crit}, must also be known to determine P_{asl}. Schulze has specified two different equations for h_{crit} (19, 33), which are functions of the surface tension and contact angle. These equations appear to also be system dependent. Schulze (5) has also indicated that h_0 is a function of particle diameter, fluid viscosity, particle settling velocity, surface tension, and surface mobility, and this function depends on the specific system of interest. Rulev and Dukhin (10) concluded that both h_0 and h_{crit} are functions of the surface tension and collision process. For quasi-elastic collisions ($St > 1$, where St is the Stokes number), they indicate that $h_0/h_{crit} \approx 3$. For inelastic collisions ($0.1 < St \leq 1$), $h_0/h_{crit} \approx 4$. Therefore, although we do not know the specific values of h_0 or h_{crit}, the ratio h_0/h_{crit} will typically be on the order of 3 to 4.

Figure 6 reveals P_{asl} predictions for a range of h_0/h_{crit} values for selected particle radii. Although Schulze (5) and Rulev and Dukhin (10) have indicated that $h_0 = f(R_p)$, we have assumed that h_0/h_{crit} is independent of R_p for these calculations. The bubble radius and particle density were fixed at 0.5 mm and 1.3 g/cm^3, respectively. There is not much difference between the results when $R_p \leq 100\ \mu m$, but at $R_p = 200$, 300, and 500 μm, P_{asl} increases considerably for a fixed h_0/h_{crit}. This is due to the particle no longer following Stokes flow and deviating from the fluid streamlines. This will be further discussed below. As h_0/h_{crit} increases, there is a sharp decrease in P_{asl} (note the figure has a log-log scale). If $h_0/h_{crit} > 5$, $P_{asl} \leq 0.001$ when $R_p < 100\ \mu m$ and particle attachment is unlikely (a chance of less than 1 in 1000). The range specified by Rulev and Dukhin (9), $3 \leq h_0/h_{crit} \leq 4$, does provide a reasonable estimate for P_{asl}.

Figure 7 shows the resulting P_{asl} predictions for $h_0/h_{crit} = 4$ and $\rho_p = 1.3\ g/cm^3$. The large filled circles on the $R_p = 200$, 300, and 500 μm curves represent conditions when $R_p = R_B$, values where the calculations are terminated (i.e., the model is valid for $R_p \leq R_B$). When $1\ \mu m \leq R_p \leq 100\ \mu m$, a local minimum in P_{asl} is observed at $R_B \approx 0.5\ mm$, then P_{asl} increases with increasing R_B. Increasing the particle radius to $R_p = 200\ mm$ increases P_{asl} and reveals similar trends, but the local minimum is not very pronounced. Further increases in the particle radius to $R_p = 300$ and 500 μm reduces the sensitivity of P_{asl} to the bubble radius, with $R_p = 500\ \mu m$ revealing P_{asl} is nearly independent of R_B at these particle radii for $0.5\ mm \leq R_B \leq 5\ mm$.

The particle radius was varied between $1\ \mu m \leq R_p \leq 500\ \mu m$ to determine its influence on P_{asl} at selected bubble radii. Figure 8 shows the predicted P_{asl} values for $h_0/h_{crit} = 4$ and $\rho_p = 1.3\ g/cm^3$. The two large filled circles on the $R_B = 0.1$ and 0.3 mm curves correspond to R_p values (100 and 300 μm) where the calculations were terminated to satisfy $R_p \leq R_B$. Figure 8 has a sharp transition when $\rho_p = 1.3\ g/cm^3$ at $R_p \approx 112\ \mu m$. This transition corresponds to the particle radius at which the particle settling velocity transitions from

Stokes flow to non-Stokes flow, and is a function of particle density (e.g., see Fig. 3). If the particle density is decreased, the transition would be delayed to a larger particle radius. In contrast, increasing the particle density would cause the transition to occur at a smaller particle radius. This translates into a sharp rise in P_{asl} because a particle settling under non-Stokes flow conditions will cross fluid streamlines and increase the rate of film thinning between a bubble and particle, thereby increasing P_{asl}.

When $R_p \leq 112\ \mu m$, $R_B = 0.5\ mm$ results in a minimum P_{asl} for all considered bubble radii. Also, there is only a small effect on P_{asl} when the bubble radius varies from 0.1 mm to 1 mm. For these conditions, increasing R_p increases P_{asl} slightly. When $R_p \geq 112\ \mu m$, increasing R_p increases P_{asl} considerably and P_{asl} is nearly independent of R_B for $0.1\ mm \leq R_B \leq 1\ mm$. When $R_B = 3$ or $5\ mm$, P_{asl} is much larger, but the transition at $R_p \approx 112\ \mu m$ is still observed. For these bubble radii (and particle density), P_{asl} is approximately independent of R_p for $R_p \leq 112\ \mu m$ and increases with increasing R_p for $R_p \geq 112\ \mu m$. For all bubble radii considered, P_{asl} asymptotes to the same value at $R_p = 500\ \mu m$.

Particle density affects P_{asl} through the dimensionless particle settling velocity, G, and through the dimensionless friction factor, λ. To determine the sensitivity of P_{asl} to particle density, calculations were completed for $1\ g/cm^3 \leq \rho_p \leq 3\ g/cm^3$ with $h_0/h_{crit} = 4$. This particle density range encompasses particles expected in flotation deinking applications, where toner particles typically have a density in the range of $1.1 - 1.6\ g/cm^3$ (30).

Figure 9 reveals P_{asl} as a function of particle density for selected particle radii at $R_B = 0.5\ mm$ and $h_0/h_{crit} = 4$. For all particle radii, increasing the particle density increases P_{asl}, which is reasonable because a heavier particle will cross fluid streamlines and increase the thinning rate of the liquid film separating the particle from the bubble. For $R_p = 1$, 10, and 50 μm, this increase is smooth and continuous because the particle is settling under

Stokes flow conditions for all particle densities considered. When $R_p = 100\ \mu m$, there is a discontinuity in the P_{asl} predictions at $\rho_p \approx 1.4\ g/cm^3$, which corresponds to the particle deviation from Stokes flow (i.e., see Fig. 3 - note the scales are different). This deviation causes P_{asl} to increase more than if the particle was settling under Stokes flow conditions. At $R_p = 200$, 300, and 500 μm, the deviation from Stokes flow occurs at low particle densities ($\rho_p < 1.1\ g/cm^3$), which causes P_{asl} to increase substantially as the particle density increases, and then asymptote to a constant value depending on R_p. This corresponds to λ asymptoting to a constant as a function of R_p in Fig. 3.

Conclusions

A closed-form approximate analytical expression for the probability of attachment by sliding has been developed in this paper. This expression, the first of its kind, accounts for the effect of interfacial tension on the disjoining film for both Stokes and non-Stokes flow conditions, and assumes that the bubble and particle are spherical with $R_p \leq R_B$. Future extensions of this approximation could include London-Van der Waals dispersion forces, electrostatic interactions, and/or long-range hydrophobic attraction forces.

The model can be used to determine P_{asl} as a function of fluid properties, bubble and particle physical properties, and the ratio h_0/h_{crit} (which has been shown in the literature to vary between 3 and 4). Therefore, the probability of this important microprocess can be determined from a rather simple expression when these flotation characteristics are known. This is a large improvement over what was previously available in the literature for P_{asl}.

Selected P_{asl} predictions have also been presented in this paper using our new expression and encompassed the ranges $1 < h_0/h_{crit} \leq 100$, $0.1\ mm \leq R_B \leq 5\ mm$, $1\ \mu m \leq R_p \leq 500\ \mu m$, and $1\ g/cm^3 < \rho_p \leq 3\ g/cm^3$. In general, P_{asl} decreases with increasing h_0/h_{crit}

and increases with increasing R_B, R_p, and ρ_p. Deviations in these general trends produce local minima in the predictions. The particle settling velocity was shown to be an important parameter and, when deviations from Stokes flow exist, a sharp transition results, with P_{asl} increasing considerably.

Acknowledgment

The work described in this paper was funded by the Member Companies of the Institute of Paper Science and Technology. Their continued support is gratefully acknowledged.

Nomenclature

Ar - Archimedes number

$A(r)$ - Eq. [53]

C_B - measure of bubble surface mobility

C_D - coefficient of drag (for a particle)

C_D^{st} - coefficient of drag in Stokes flow

d_B - bubble diameter

d_p - particle diameter

F_c - magnitude of the centrifugal force exerted on a particle

F_{gr} - magnitude of the radial component of the particle weight

$F_{g\varphi}$ - magnitude of the tangential component of the particle weight

F_{ur} - magnitude of the flow force in the radial direction acting on a particle in the vicinity of the bubble surface

$F_{u\varphi}$ - magnitude of the flow force in the tangential direction acting on a particle in the vicinity of the bubble surface

$F_{w\varphi}$ - magnitude of the drag force in the tangential direction acting on the particle in the vicinity of the bubble surface

$\tilde{F}_{w\varphi}$ - magnitude of the force $F_{w\varphi}$ for the case of a Stokes flow about the bubble

F_L - magnitude of the lift force acting on a particle

F_T - magnitude of the resistive force generated during the drainage of the disjoining film

$\mathbf{F}_d$ - drag force acting on a particle

f - friction factor

G - dimensionless particle settling velocity $\left(= \lambda \frac{\tilde{v}_{ps}}{v_B} \equiv \frac{v_{ps}}{v_B} \right)$

$\tilde{G}$ - G for the case of Stokes flow about the bubble

g - acceleration due to gravity

$g(r)$ - Eq. [26]

$\tilde{g}(r)$ - $g(r)$ for Stokes flow

$g'(r)$ - Eq. [34]

$h(x,t)$ - height of the disjoining film at the position $x = R_B\varphi$ along the bubble surface

h_{crit} - critical film thickness at rupture

h_0 - $(h_p(0))$, disjoining film thickness at the instant of contact with the particle

$h_p(t)$ - thickness of the disjoining film below the current position of the particle at time t

$\bar{h}_p$ - $(h_p(t) - h_0)$

$k(r)$ - Eq. [40]

$\tilde{k}(r)$ - $k(r)$ for Stokes flow

L -	length of the particle sliding path
P_{asl} -	microprocess probability of adhesion by sliding
$\tilde{P}_{asl}$ -	P_{asl} for Stokes flow
P_σ -	disjoining pressure
Q -	Eq. [55]
Re_p -	particle Reynolds number
Re_S -	Reynolds number of shear
Re_B -	bubble Reynolds number
Re_B^* -	$\left(\frac{1}{15}Re_B^{0.72}\right)$
R_p -	particle radius
R_B -	bubble radius
R_T -	touching radius from stagnation streamline (Fig. 2)
r -	radial distance of a particle from a bubble
$r_p(t)$ -	$(R_B + R_p + h_p(t))$, the radial position
St -	Stokes number $\frac{\rho_p d_p^2 v_B}{9\mu_\ell d_B}$
t -	time
u_r -	radial component of the fluid velocity
u_φ -	angular component of the fluid velocity
$\mathbf{v}_p$ -	particle velocity
$v_{p\varphi}^{rel}$ -	$(u_\varphi - v_{ps}\sin\varphi_p)$
v_{pr} -	radial component of the particle velocity
$v_{p\varphi}$ -	tangential component of the particle velocity

$\mathbf{v}_{ps}$ - particle settling velocity

v_{ps} - magnitude of the particle settling velocity

$\tilde{v}_{ps}$ - magnitude of the particle settling velocity in Stokes flow

v_B - bubble rise velocity

x - distance along bubble surface from the stagnation point ($= R_B\varphi$)

$\triangle\rho$ - $(\rho_p - \rho_\ell)$

λ - dimensionless friction factor ($= 6\pi\mu_\ell R_p/f$)

μ_ℓ - fluid viscosity

ν_ℓ - kinematic fluid viscosity

ρ_ℓ - fluid density

ρ_p - particle density

σ - surface tension

τ_i - fluid film induction time

τ_{sl} - particle sliding time

$\varphi_p(t)$ - angular position of the particle at time t

φ_T - particle touching angle ($= \varphi_p(0) = \varphi_0$)

φ_{crit} - angular position at which film rupture occurs

φ^*_{crit} - largest value of φ_T, for a given h_0, such that film rupture will occur at an angle $\varphi = \varphi_{crit} \leq \pi/2$

Φ_p - mapping of $\varphi_0 \longrightarrow \varphi_{crit}$ at an arbitrary value of h_0

Φ_{p,h_0} - Φ_p at a fixed value of h_0

Φ^{-1}_{p,h_0} - inverse map to Φ_{p,h_0}

References

1. Bloom, F. and Heindel, T.J., *Mathl. Comput. Modelling* **25**, 13 (1997).
2. Bloom, F. and Heindel, T.J., *J. Colloid Interface Sci.* **190**, 182 (1997).
3. Heindel, T.J., *TAPPI J.* **82** (3), 115 (1999).
4. Schulze, H.J., "Physicochemical Elementary Processes in Flotation." Elsevier, Amsterdam, 1984.
5. Schulze, H.J., *in* "Coagulation and Flocculation"(B. Dobias, Ed.), p. 321. Marcel Dekker, New York, 1993.
6. Yoon, R.H., and Mao, L., *J. Colloid Interface Sci.* **181**, 613 (1996).
7. Yoon, R.H. and Luttrell, G.H., *Miner. Process. Extract. Metal. Rev.* **5,** 101 (1989).
8. Heindel, T.J. and Bloom, F., *J. Colloid Interface Sci.* **213**, 101 (1999).
9. Derjaguin, B.V., Dukhin, S.S., and Rulev, N.N., *Colloid Journal of the USSR*, Part I, **39**, 926 (1978).
10. Rulev, N.N. and Dukhin, S.S., *Kolloidnyi Zhurnal* **48**, 302 (1986).
11. Ruckenstein, E. and Jain, R., *J.C.S. Foraday II* **66**, 132 (1970).
12. Scheludko, A., Toshev, B.V., and Bojadjiev, D.T., *J. Chem. Soc. Trans. Faraday* **72**, 2815 (1976).
13. Jain, R. and Ivanov, I.B., *J.C.S. Faraday II* **76**, 250 (1980).
14. Williams, M.B., and Davis, S.H., *J. Colloid Interface Sci.* **90**, 220 (1982).
15. Paulsen, F.G., Pan, R., Bousfield, D., and Thompson, E., *in* "2nd Research Forum on Recycling," p. 1. TAPPI Press, Atlanta, 1993.
16. Paulsen, F.G., Bousfield, D.W., and Thompson, E.V., *in* "1996 Pulping Conference Proceedings," p. 145. TAPPI Press, Atlanta, 1996.
17. Nguyen, A.V., Schulze, H.J. and Ralston, J., *Int. J. Miner. Process.* **51**, 183 (1997).
18. Nguyen, A.V., Ralston, J. and Schulze, H.J., *Int. J. Miner. Process.* **53**, 225 (1998).
19. Schulze, H.J., *Adv. in Colloid Interface Sci.* **40**, 283 (1992).
20. Dobby, G.S. and Finch, J.A., *J. Colloid Interface Sci.* **109**, 493 (1986).

21. Cheremisinoff, M.P., *in* "Encyclopedia of Fluid Mechanics, 5: Slurry Flow Technology," (N.P. Cheremisinoff, Ed.), p. 686. Gulf Publishing Company, London, 1986.

22. Goldman, A.J., Cox, R.G., and Brenner, H., *Chem. Eng. Sci.* **22**, 637 (1967).

23. Saffman, P.G. *J. Fluid Mech.* **22**, 385 (1965).

24. Clift, R., Grace, J.R., and Weber, M.E., "Bubbles, Drops, and Particles." Academic Press, Inc., New York, 1978.

25. Mileva, E., *Colloid Polym. Sci.* **268**, 375 (1990).

26. Moore, D.W., *J. Fluid Mech* **16**, 161 (1963).

27. Luttrell, G.H. and Yoon, R.H., *J. Colloid Interface Sci.* **154**, 129 (1992).

28. Schulze, H.J. and Gottschalk, G., *in* "Proceedings of the 13th Int. Min. Proc. Congr.," (J. Laskowski, Ed.) p. 63. Elsevier, New York, 1981.

29. McLaughlin, J.B., *J. Fluid Mech.* **224**, 261 (1991).

30. Vidotti, R.M., Johnson, D.A., and Thompson, E.V., *Prog. Pap. Recycl.* **2**, 30 (1993).

31. Heindel, T.J., and Monefeldt, J.L., *Tappi J.* **81** (11), 149 (1998).

32. Heindel, T.J., *J. Pulp Pap. Sci.* **25**, 104 (1999).

33. Schulze, H.J., *in* "1st Research Forum on Recycling," p. 161. CPPA Press, Toronto, 1991.

Figure Captions

Figure 1: The forces acting on a particle as it slides over a bubble surface.

Figure 2: Physical interpretation of $\varphi_p(t)$ and $h_p(t)$.

Figure 3: Effect of particle density, ρ_p, on the dimensionless particle friction factor, λ, for selected particle radii, R_p.

Figure 4: Comparison of the terms in [35].

Figure 5: The magnitudes of various forces as a function of particle radius, R_p.

Figure 6: P_{asl} as a function of h_0/h_{crit} for selected particle radii, R_p, with $R_B = 0.5\ mm$ and $\rho_p = 1.3\ g/cm^3$.

Figure 7: P_{asl} as a function of bubble radius, R_B, for selected particle radii, R_p, with $h_0/h_{crit} = 4$ and $\rho_p = 1.3\ g/cm^3$.

Figure 8: P_{asl} as a function of particle radius, R_p, for selected bubble radii, R_B, with $h_0/h_{crit} = 4$ and $\rho_p = 1.3\ g/cm^3$.

Figure 9: P_{asl} as a function of particle density, ρ_p, for selected particle radii, R_p, with $R_B = 0.5\ mm$ and $h_0/h_{crit} = 4$.

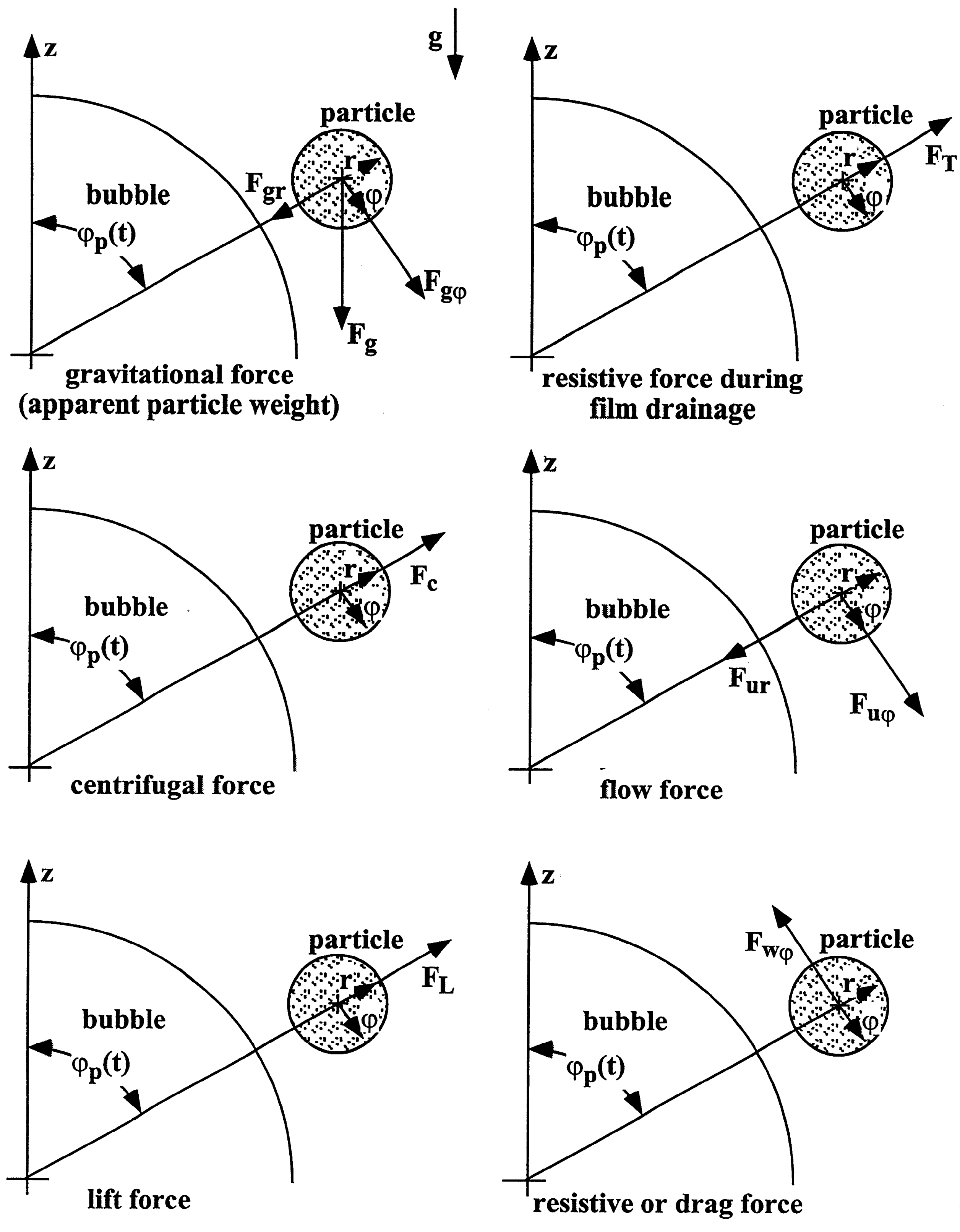
z
g
particle
bubble
Fgr
r
φ
φp(t)
Fgφ
Fg
gravitational force
(apparent particle weight)
z
particle
FT
bubble
r
φ
φp(t)
resistive force during
film drainage
z
particle
bubble
r
Fc
φ
φp(t)
centrifugal force
z
particle
bubble
r
φ
φp(t)
Fur
Fuφ
flow force
z
particle
bubble
r
FL
φ
φp(t)
lift force
z
Fwφ
particle
bubble
r
φ
φp(t)
resistive or drag force

Figure 1

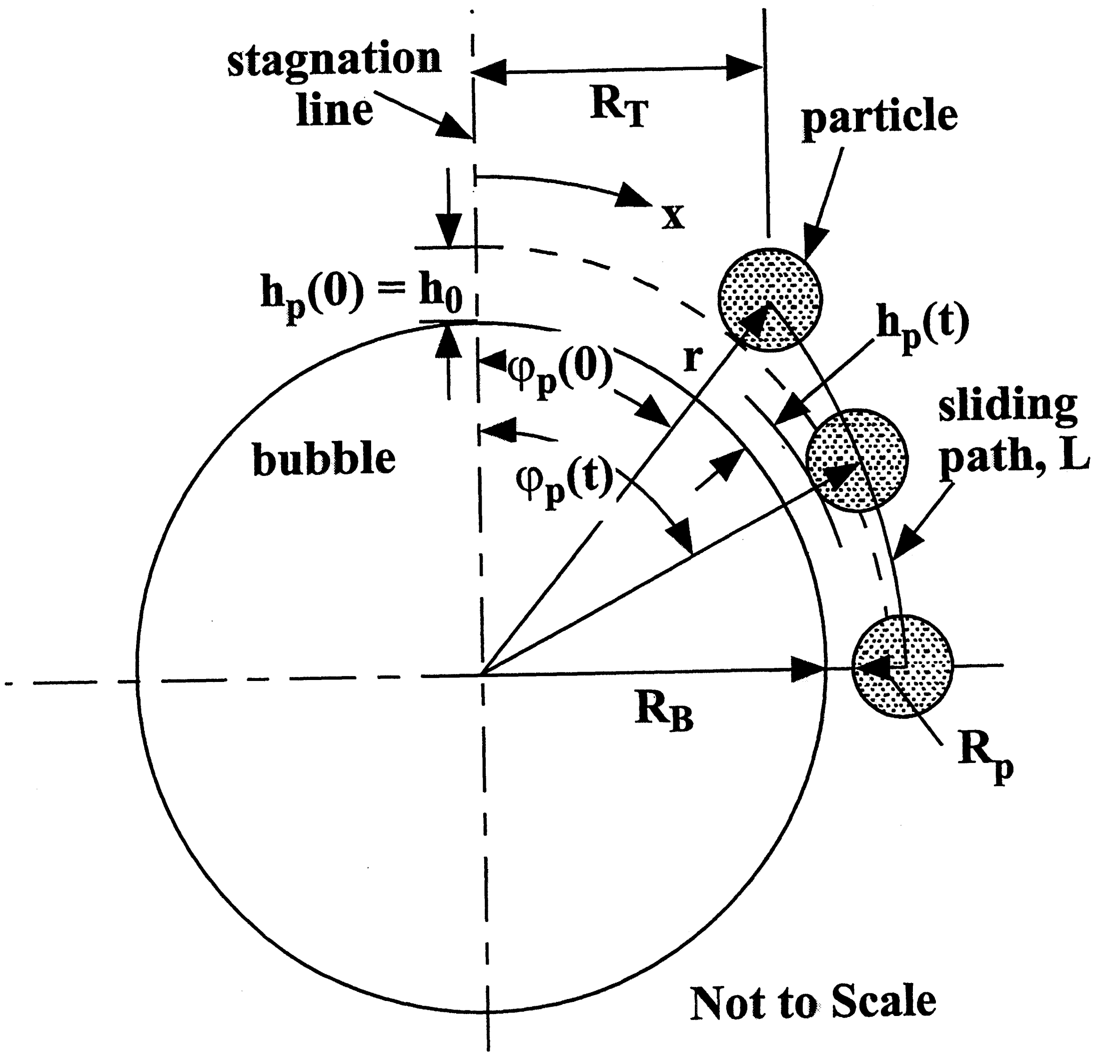
stagnation
line
R_T
particle
x
$h_p(0) = h_0$
$h_p(t)$
r
$\varphi_p(0)$
sliding
path, L
bubble
$\varphi_p(t)$
R_B
R_p
Not to Scale

Figure 2

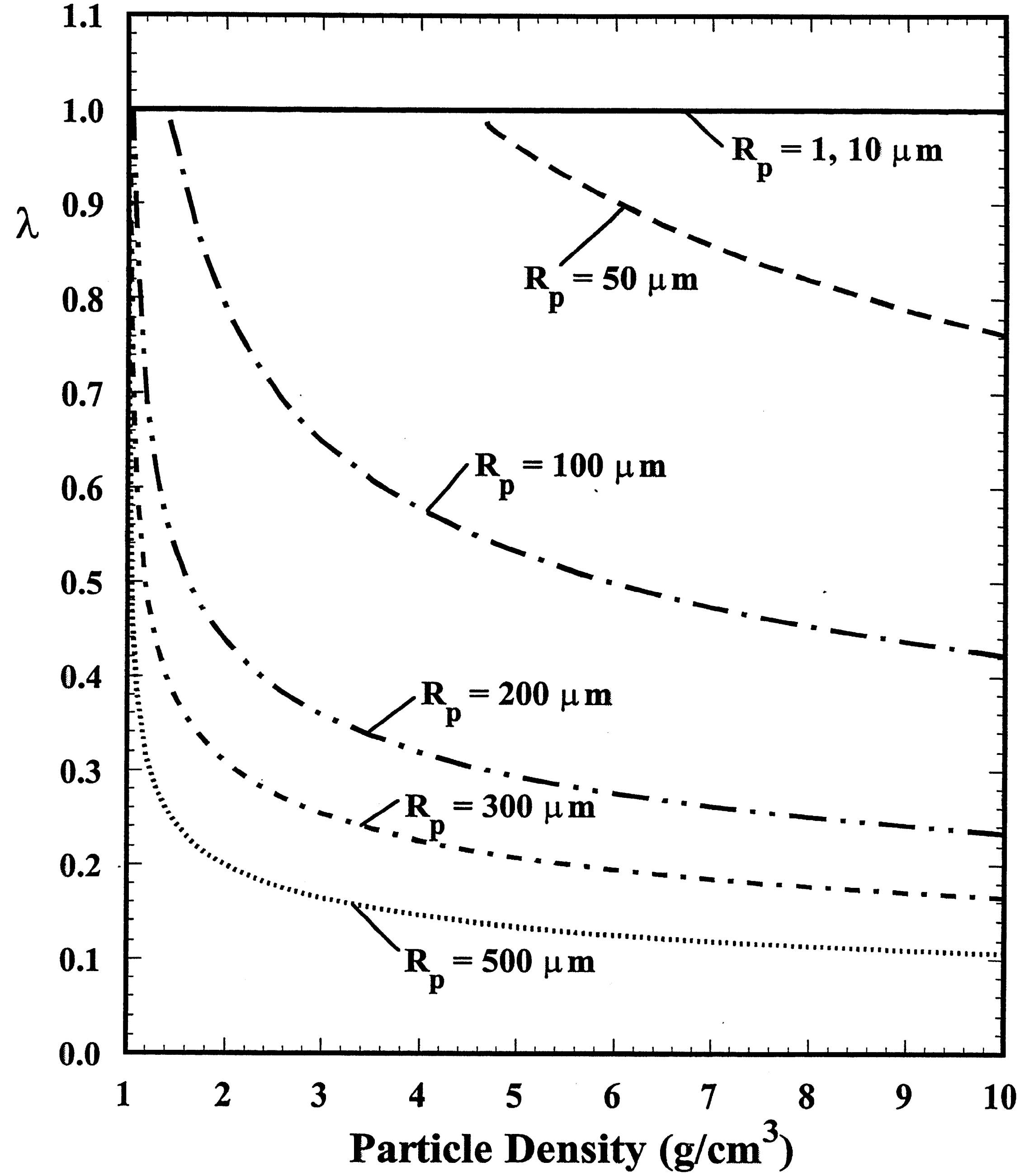

1.1
1.0
0.9
0.8
0.7
0.6
0.5
0.4
0.3
0.2
0.1
0.0
λ
1
2
3
4
5
6
7
8
9
10
Particle Density (g/cm3)
Rp = 1, 10 μm
Rp = 50 μm
Rp = 100 μm
Rp = 200 μm
Rp = 300 μm
Rp = 500 μm

Figure 3

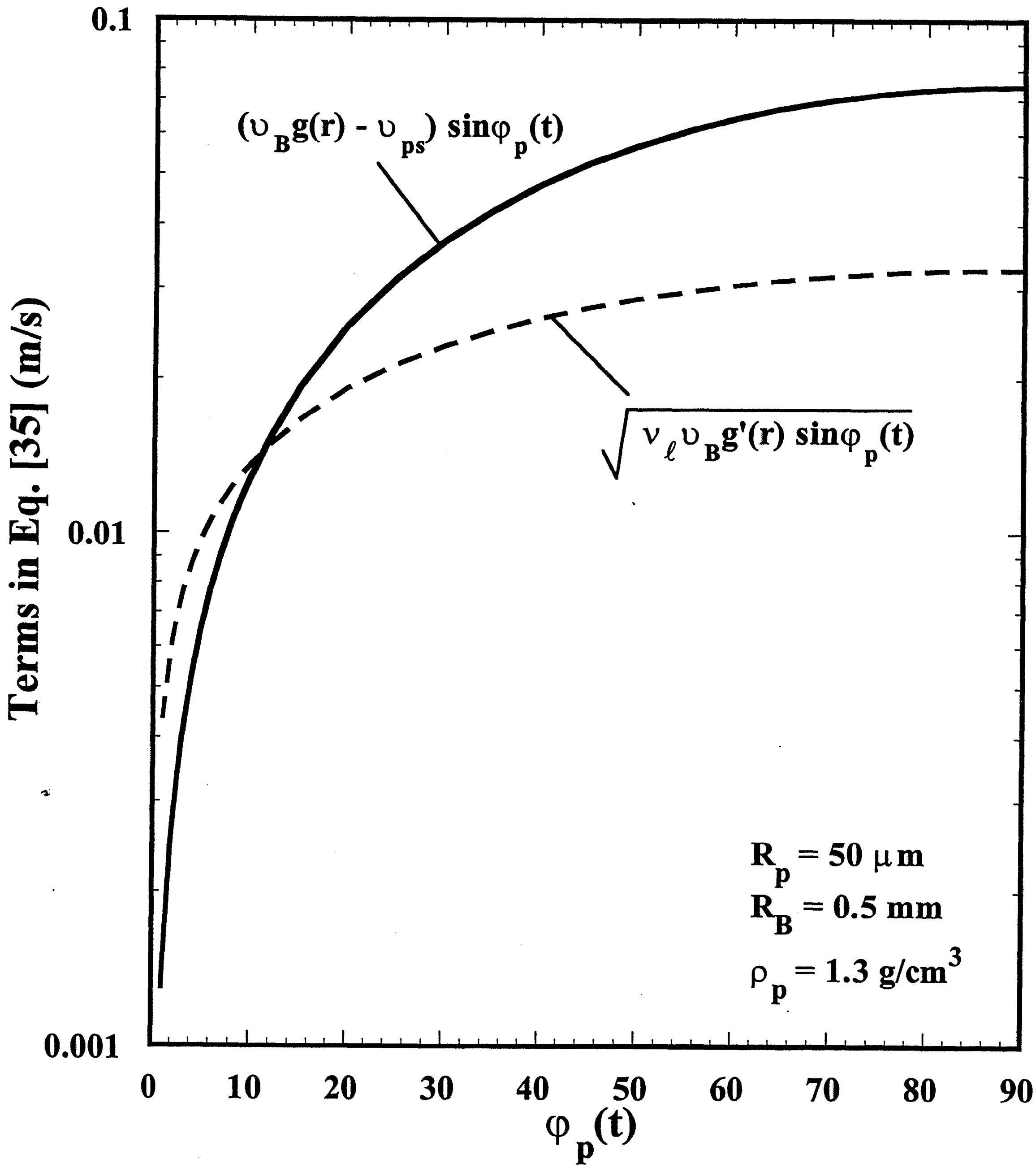
0.1
0.01
0.001
Terms in Eq. [35] (m/s)
$(\upsilon_B g(r) - \upsilon_{ps}) \sin\varphi_p(t)$
$\sqrt{\nu_\ell \upsilon_B g'(r) \sin\varphi_p(t)}$
$R_p = 50\ \mu m$
$R_B = 0.5$ mm
$\rho_p = 1.3\ g/cm^3$
0
10
20
30
40
50
60
70
80
90
$\varphi_p(t)$

Figure 4

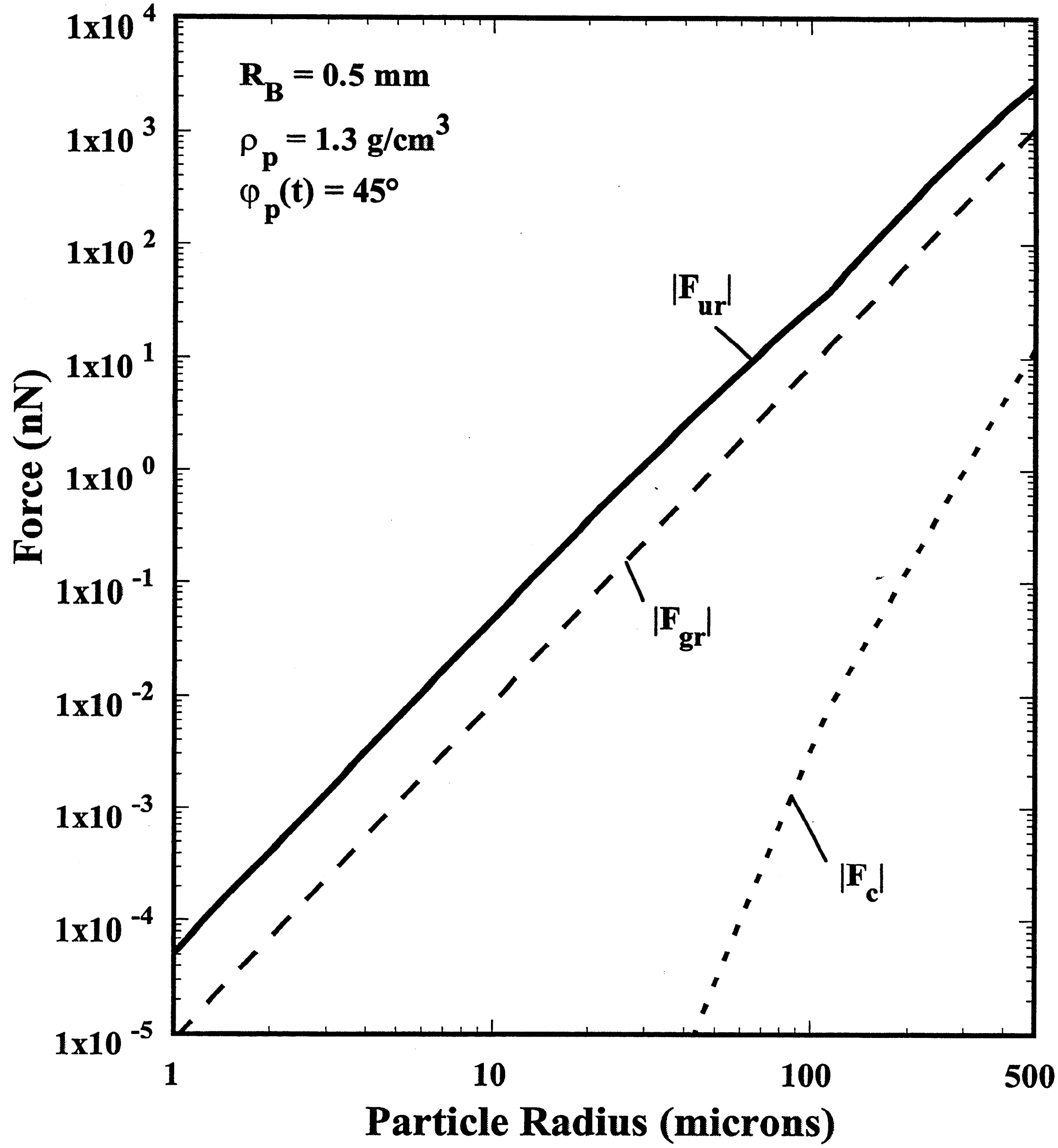
R_B = 0.5 mm
ρ_p = 1.3 g/cm^3
$\varphi_p(t)$ = 45°
$|F_{ur}|$
$|F_{gr}|$
$|F_c|$
Force (nN)
$1x10^{4}$
$1x10^{3}$
$1x10^{2}$
$1x10^{1}$
$1x10^{0}$
$1x10^{-1}$
$1x10^{-2}$
$1x10^{-3}$
$1x10^{-4}$
$1x10^{-5}$
1
10
100
500
Particle Radius (microns)

Figure 5

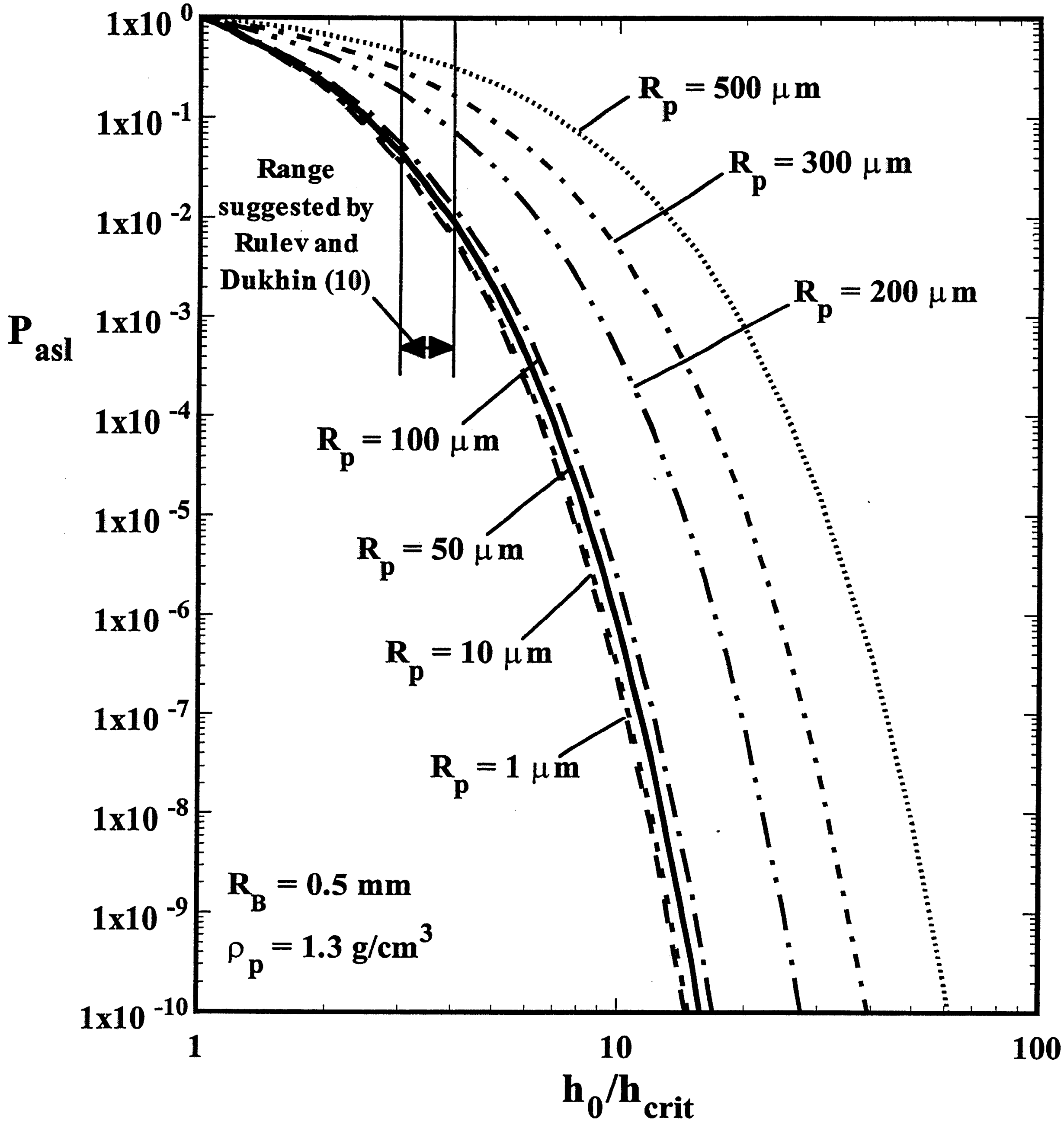

1x10 0
1x10 -1
1x10 -2
1x10 -3
1x10 -4
1x10 -5
1x10 -6
1x10 -7
1x10 -8
1x10 -9
1x10 -10
P asl
1
10
100
h0/hcrit
Range suggested by Rulev and Dukhin (10)
Rp = 500 μm
Rp = 300 μm
Rp = 200 μm
Rp = 100 μm
Rp = 50 μm
Rp = 10 μm
Rp = 1 μm
RB = 0.5 mm
ρp = 1.3 g/cm3

Figure 6

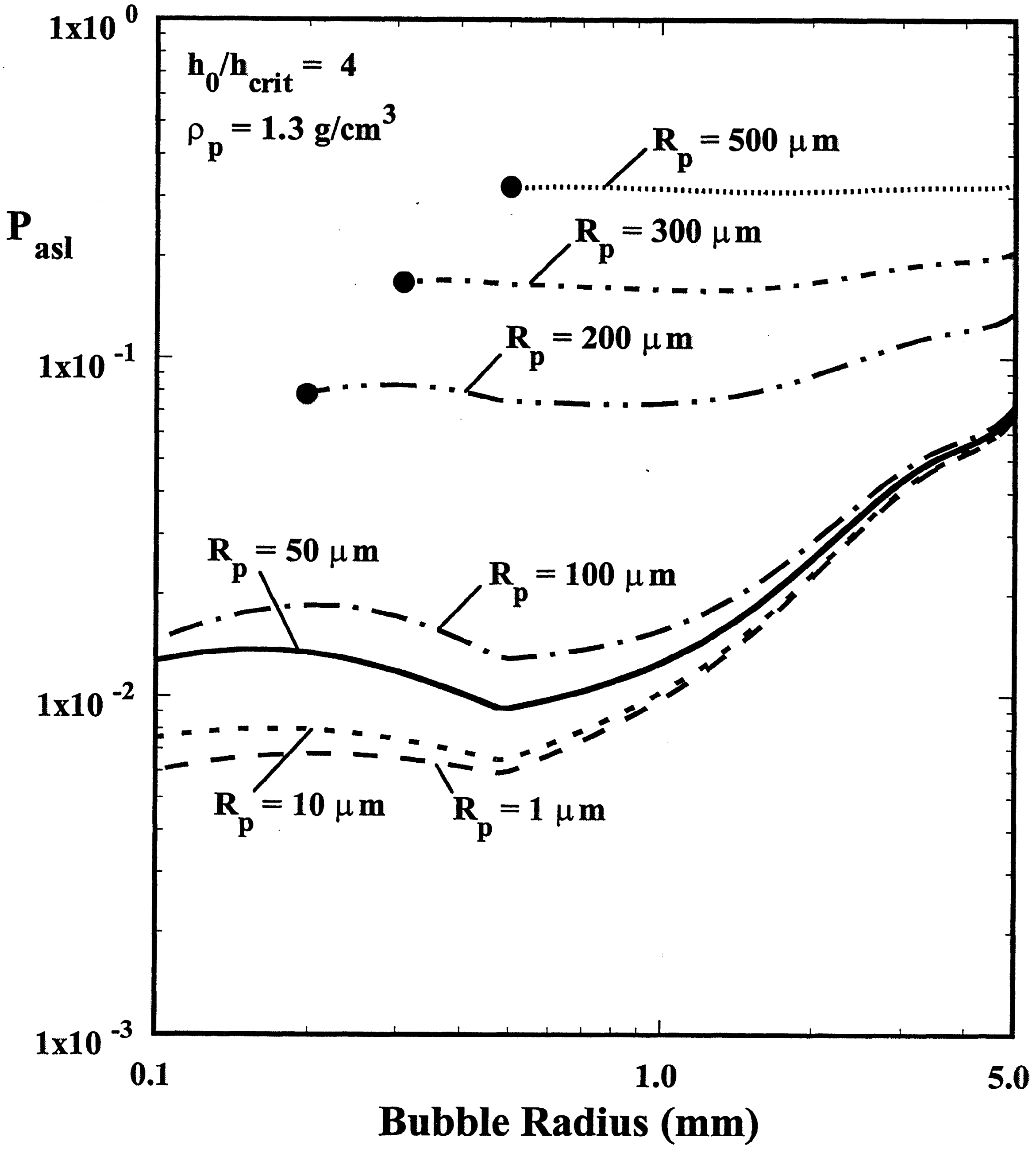

1x10 0
1x10 -1
1x10 -2
1x10 -3
P asl
h0/hcrit = 4
ρp = 1.3 g/cm3
Rp = 500 µm
Rp = 300 µm
Rp = 200 µm
Rp = 50 µm
Rp = 100 µm
Rp = 10 µm
Rp = 1 µm
0.1
1.0
5.0
Bubble Radius (mm)

Figure 7

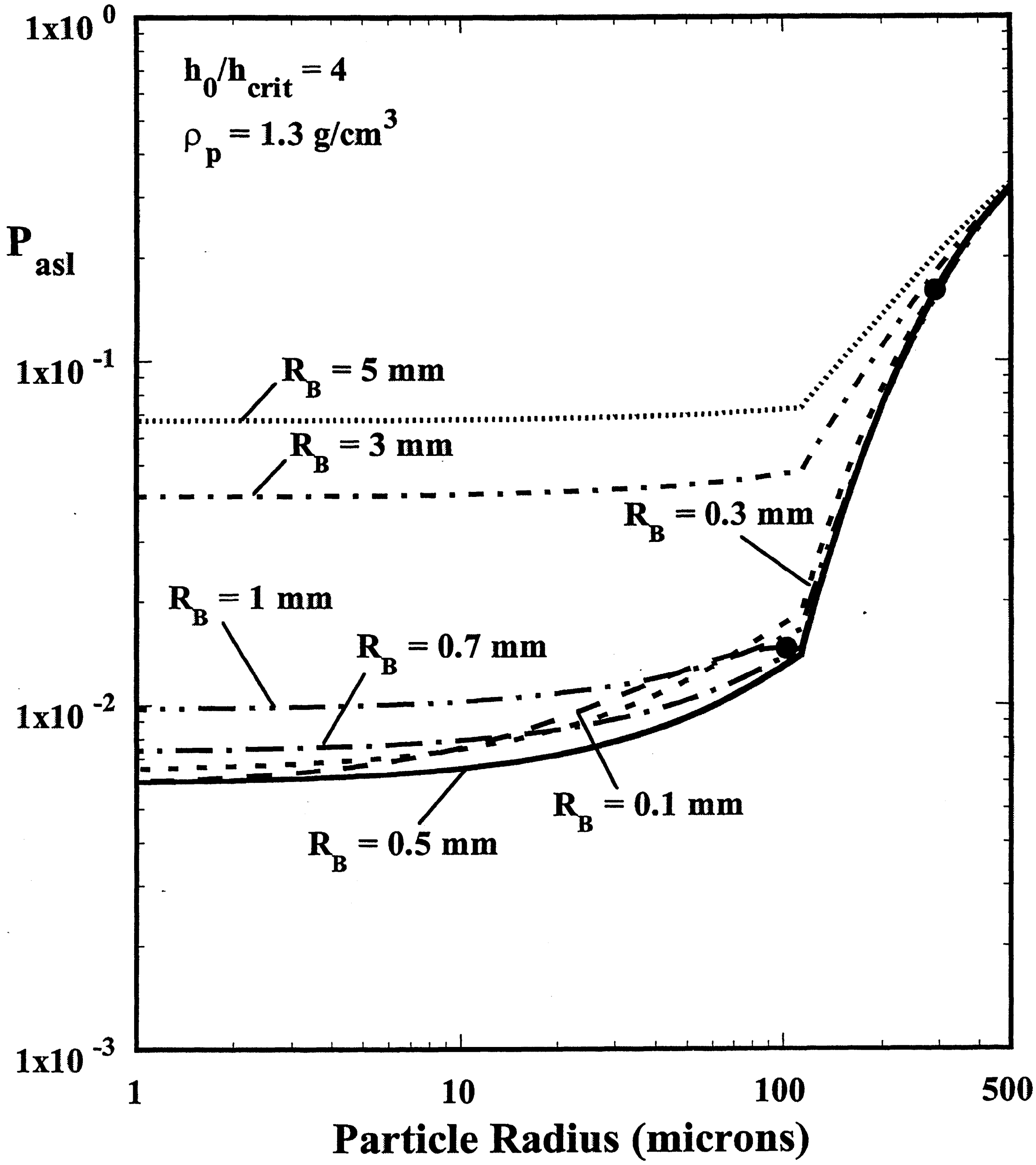

$h_0/h_{crit} = 4$
$\rho_p = 1.3$ g/cm^3
P_{asl}
$R_B = 5$ mm
$R_B = 3$ mm
$R_B = 0.3$ mm
$R_B = 1$ mm
$R_B = 0.7$ mm
$R_B = 0.1$ mm
$R_B = 0.5$ mm
1x10 ^{0}
1x10 $^{-1}$
1x10 $^{-2}$
1x10 $^{-3}$
1
10
100
500
Particle Radius (microns)

Figure 8

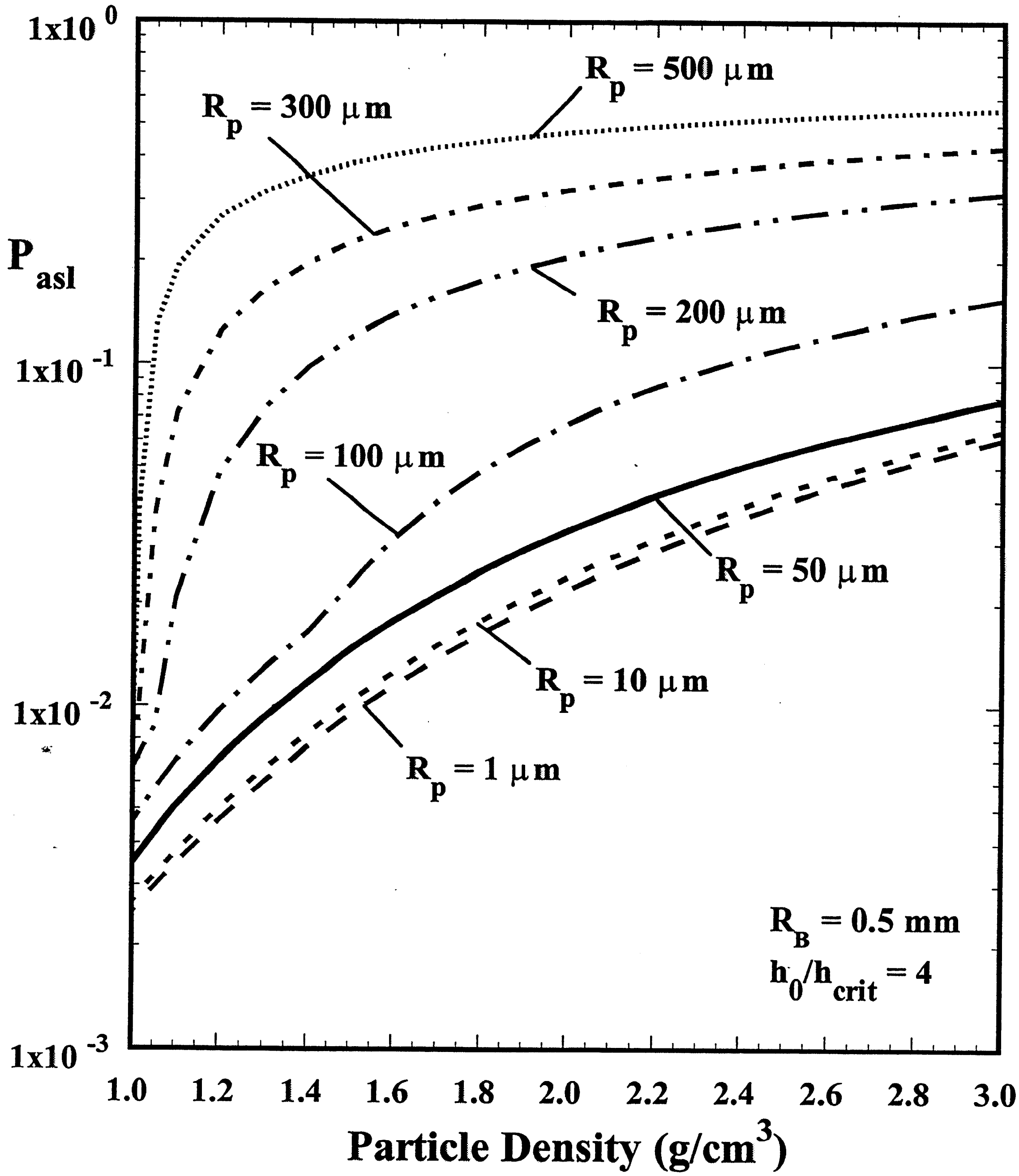
1x10 0
1x10 -1
1x10 -2
1x10 -3
P asl
R p = 500 µm
R p = 300 µm
R p = 200 µm
R p = 100 µm
R p = 50 µm
R p = 10 µm
R p = 1 µm
R B = 0.5 mm
h 0/h crit = 4
1.0
1.2
1.4
1.6
1.8
2.0
2.2
2.4
2.6
2.8
3.0
Particle Density (g/cm3)

Figure 9